This is the accepted manuscript made available via CHORUS. The article has been published as:

Laser-induced quenching of metastability at the Mott insulator to metal transition

Theodor Luibrand, Lorenzo Fratino, Farnaz Tahouni-Bonab, Amihai Kronman, Yoav Kalcheim, Ivan K. Schuller, Marcelo Rozenberg, Reinhold Kleiner, Dieter Koelle, and Stefan Guénon

Phys. Rev. B **110**, L081108 — Published 14 August 2024

DOI: 10.1103/PhysRevB.110.L081108

Laser-induced quenching of metastability at the Mott-insulator to metal transition

Theodor Luibrand,[1] Lorenzo Fratino,[2,3] Farnaz Tahouni-Bonab,[1] Amihai Kronman,[4] Yoav Kalcheim,[4,5] Ivan K. Schuller,[5] Marcelo Rozenberg,[3] Reinhold Kleiner,[1] Dieter Koelle,[1] and Stefan Guénon[1,*]

[1] *Physikalisches Institut, Center for Quantum Science (CQ) and LISA$^+$, Eberhard Karls Universität Tübingen, Auf der Morgenstelle 14, 72076 Tübingen, Germany*

[2] *CNRS Laboratoire de Physique Théorique et Modélisation, CY Cergy Paris Université, 95302 Cergy-Pontoise Cedex, France*

[3] *CNRS Laboratoire de Physique des Solides, Université Paris-Saclay, 91405, Orsay, France*

[4] *Department of Materials Science and Engineering, Technion – Israel Institute of Technology, Technion City, 32000 Haifa, Israel*

[5] *Center for Advanced Nanoscience, Department of Physics, University of California — San Diego, 9500 Gilman Drive, La Jolla, CA92093-0319, USA*

There is growing interest in strongly correlated insulator thin films because the intricate interplay of their intrinsic and extrinsic state variables causes memristive behavior that might be used for bio-mimetic devices in the emerging field of neuromorphic computing. In this study we find that laser irradiation tends to drive V_2O_3 from supercooled/superheated metastable states towards thermodynamic equilibrium, most likely in a non-thermal way. We study thin films of the prototypical Mott-insulator V_2O_3, which show spontaneous phase separation into metal-insulator herringbone domains during the Mott transition. Here, we use low-temperature microscopy to investigate how these metal-insulator domains can be modified by scanning a focused laser beam across the thin film surface. We find that the response depends on the thermal history: When the thin film is heated from below the Mott transition temperature, the laser beam predominantly induces metallic domains. On the contrary, when the thin film is cooled from a temperature above the transition, the laser beam predominantly induces insulating domains. Very likely, the V_2O_3 thin film is in a superheated or supercooled state, respectively, during the first-order phase transition, and the perturbation by a laser beam drives these metastable states into stable ones. This way, the thermal history is locally erased. Our findings are supported by a phenomenological model with a laser-induced lowering of the energy barrier between the metastable and equilibrium states.

Strongly correlated insulator thin films are the subject of intensive research in the emerging field of neuromorphic computing [1–4]. If these materials are cooled to a temperature below the transition temperature, the charge carrier mobility is considerably reduced due to electron-electron correlation effects like the Mott-Hubbard interaction (e.g., V_2O_3 [5–9]), charge transfer (e.g., rare-earth nickelates [10, 11]) or dimerization (e.g., VO_2)[12]. This reduction in charge carrier mobility results in a metal-to-insulator transition (MIT) [13]. An equivalent insulator-to-metal transition (IMT) is observed during heating. The electron-electron correlation effects cause an intricate interplay of intrinsic and extrinsic state variables that can be leveraged for engineering neuromorphic devices [14]. One way to influence strongly correlated insulator thin-film devices externally is through exposure to light. For instance, light is used to trigger resistive switching [15–18], to tune the resistive switching voltage thresholds [19] or to tune the frequency of relaxation oscillators [20] in VO_2 devices. Furthermore, because strongly correlated insulator thin-film neuromorphic devices are usually operated in a critical state at the onset of the IMT/MIT, their functionality is affected by thermodynamics of phase transitions. For instance, the hysteresis in resistance R vs temperature T curves due to the first-order MIT/IMT in VO_2 is leveraged for multistate resistive switching [21–23]. In V_2O_3, the MIT/IMT is accompanied by structural (corundum to monclinic) and magnetic (paramagnetic to antiferromagnetic) phase transitions, providing a complex interplay of many degrees of freedom [24–27].

It is widely recognized that the Mott transition in V_2O_3 is of first-order. However, the implication that the thermodynamic states must be metastable due to fundamental thermodynamics needs to be addressed. Here, we investigate how a laser induced local perturbation affects metastability in a V_2O_3 thin film. We recorded the laser light induced phase transitions at temperatures during the IMT/MIT by acquiring photomicrographs. While at the IMT, the metal phase is induced, the insulating phase is predominantly induced at the MIT. The latter is very intriguing, because one might expect the main effect of the laser irradiation to be heating, which is expected to drive the system towards a more metallic state. To study this phenomenon further, we investigated the filling factors of the insulating and metallic phases and found that after laser irradiation, the filling factors of the heating and cooling branches are almost identical. The behavior is reproduced in a phenomenological numerical model.

The sample under investigation is a continuous 300-nm-thick rf-sputtered V_2O_3 film on an r-cut sapphire substrate with gold electrodes evaporated on top (see Ref. [28] for details); Fig. 1(a) shows its $R(T)$ curve for both heating and cooling. The resistance change of four orders of magnitude at the phase transition is a sign of high film quality.

We used the same optical microscopy setup as in Lange *et al.* [29], where we have demonstrated that the change in reflectivity allows for imaging the separation of the insulating and metallic phases with 0.5 μm spatial resolution. As described in Refs. [30, 31], the setup is a cryogenic combined widefield and laser scanning microscope. The sample is mounted in vacuum on the coldfinger of a liquid Helium continuous-flow cryostat. A sketch of the experimental setup is shown in Fig. 1(b), and a detailed description is given in Ref. [32] (Sec. I).

For this study, the photomicrographs are acquired in the widefield mode with an monochromatic (532 nm) LED illumination, and the laser scanning mode is used for exposing the sample under investigation to laser light from a 405 nm wavelength laser-diode operated in the continuous wave mode. The theoretical laser spot diameter on the thin-film surface is 322 nm. We have measured the incident laser power on the sample surface by replacing the sample with a photodiode. The maximum laser power is 919 μW. However, different laser powers were chosen, throughout this study.

For exposure, the selected area is scanned line by line (line separation 100 nm) as depicted in Fig. 1(b). During each line scan, the laser spot stays at a position for 13 ms then it moves to the next position at a distance of 100 nm.

The procedure to investigate the effect of laser scanning irradiation is the following:

1. A photomicrograph ($32\times32\,\mu m^2$) of the thin film is acquired.
2. A selected area ($14\times14\,\mu m^2$) is exposed to laser light.
3. A second photomicrograph is acquired.
4. For the differential image, the first photomicrograph is subtracted from the second.

With this procedure, the laser-induced changes from the metallic to the insulating and from the insulating to the metallic phases are mapped.

We have exposed a V_2O_3 thin film by laser light at different temperatures during the IMT/MIT (Fig. 1). The $R(T)$ curve shows a hysteresis of several Kelvins due to the first-oder nature of the IMT/MIT [7]. During heating of the sample from 80 K to room temperature, the heating was interrupted four times during the IMT, and a pristine (unirradiated) $14\times14\,\mu$m area was exposed with 0.1 mW laser power according to the procedure described above. The same procedure was chosen for cooling from room temperature to 80 K with 0.6 mW laser power. Note, that we chose different pristine areas on the sample for each scanning procedure.

The photomicrographs in Fig. 1(c),(d) (in particular, D and E) show the characteristic herringbone domain pattern due to strain-induced separation of the metallic and insulating phases [29, 33]. It is important to note

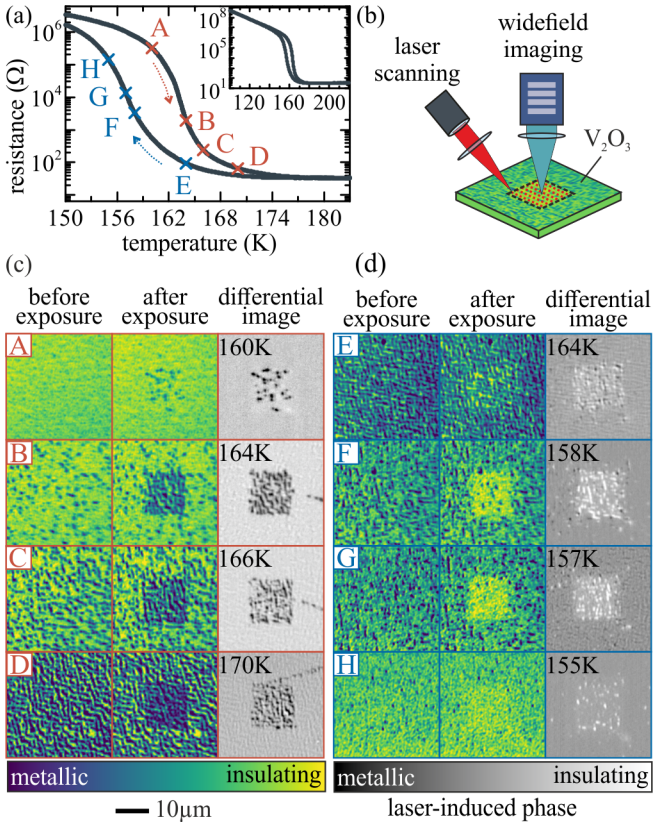


FIG. 1. (a) Zoom into the phase transition region of the $R(T)$ curve. The red and blue dashed arrows indicate the heating and cooling branch, respectively. Inset: Full $R(T)$ curve of the V_2O_3 thin film sample under investigation with same units as in the main graph. The capital letters mark the set-temperatures in one thermal cycle, at which separated squares in the V_2O_3 thin film were irradiated using the laser scanning mode. (b) Simplified schematic of the measurement setup. Photomicrographs are acquired by widefield microscopy before and after laser scanning within the dashed square of pristine areas. (c) Photomicrograph series demonstrating the laser scanning irradiation effect acquired during one heating run. For the differential images, the image before laser irradiation was subtracted from the image after scanning. The image contrasts were optimized for every temperature. (d) Photomicrograph series acquired during cooling, analogous to (c).

that these domain patterns are static on the time scale of at least 15 minutes and do not change, if the thin film is left undisturbed at a fixed temperature. The key result of this study is that during heating, mostly metallic domains are induced (dark patches in the differential images in Fig. 1(c) and (d)), whereas during cooling, predominantly insulating domains are created by laser irradiation (bright patches in the differential images in Fig. 1(c) and (d)). Furthermore, laser scanning irradiation does not smear or destroy the herringbone domain patterns but modifies them by changing the ratio of the metallic and insulating surface areas. If left undisturbed, the domains

in the irradiated areas are static for at least 10 minutes.

In an additional experiment on a patterned V_2O_3 thin film microbridge (see Fig. S2 in Ref. [32]) we show, that indeed the laser-scanning-induced phase change has a significant effect on the film resistivity. Moreover, we observe that the size of the laser-induced domains is similar to the size of the domains of the temperature-driven phase transition without laser exposure. This indicates, that domain walls permeate the whole film, and that the laser-induced phase transition is not only due to a surface effect.

We also modified the laser irradiation procedure to determine the power thresholds for laser-induced phase changes during heating and cooling (see Sec. III in Ref. [32] for details). It was found that laser irradiation already at relatively low power levels induces predominantly a metallic phase during heating (i.e., IMT), while during cooling (i.e., MIT), the required laser power for inducing predominantly an insulating phase is considerably larger. Moreover, the temperature range, in which a laser-induced phase change was observable, is larger during IMT, compared to MIT. Hence, the heating branch of the transition seems to be more sensitive to laser irradiation than the cooling branch.

For a quantitative analysis of the laser-induced phase changes, we investigated the filling factors, i.e., the ratio between the surface area of a particular phase and the total surface area of interest at a laser power of 460 μW. This laser power was chosen because it is far from the minimum and maximum threshold values for both cooling and heating (see Sec. III in Ref. [32]). As mentioned above, the metallic and insulating thin-film areas can be clearly distinguished by their brightness level in the photomicrographs (see Fig. 1 and [29]). However, these brightness levels change from micrograph to micrograph. Therefore, the following evaluation procedure was used for determining the filling factors. We visually inspected the (differential) micrographs in Fiji [34] and chose an upper and lower limit for the brightness that separates the particular two phases. A third brightness level was calculated by averaging the upper and lower limit. For these three brightness values, we calculated the filling factors, which correspond to the data points and the error bars in Fig. 2, using a Python routine.

Figure 2(a) and (b) show the temperature dependence of the filling factors of the laser-induced metallic and insulating phases during heating and cooling, respectively. Except for the fact that in the heating case, predominantly the metallic, and in the cooling case, predominantly the insulating phase is created, the overall behavior is very similar: the laser irradiation switches a considerable percentage of the thin-film area during the IMT from insulating to metallic (40% at 164 K) and during the MIT from metallic to insulating (28% at 162 K). Furthermore, in both cases, there is a temperature interval in which a smaller amount of the minor phase (insulating at the IMT and metallic at the MIT) is induced as well.

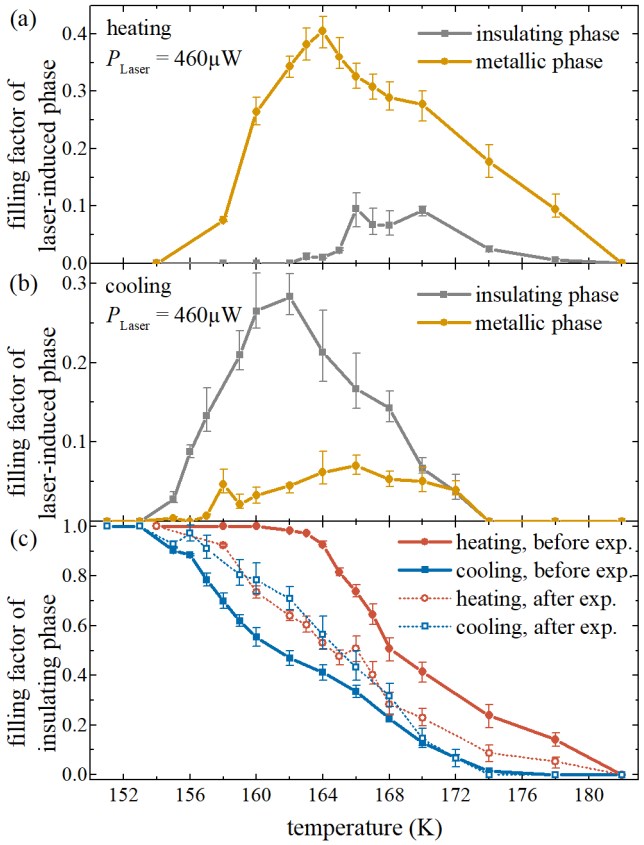


FIG. 2. Temperature dependence of metal and insulator filling factors affected by laser irradiation of 460 μW. (a) Filling factors of the metallic and insulating phases induced by laser irradiation during heating. (b) Same filling factors during cooling. (c) Filling factors of the insulating phase during one thermal cycle.

Figure 2(c) shows the filling factor of the insulating phase before and after laser irradiation. The error bars of the before-irradiation graphs are smaller compared to the after-irradiation graphs because a larger area was used for determining the filling factors before irradiation. Like the $R(T)$-curves shown in Fig. 1(a), the before-irradiation curves are hysteretic due to the first-order character of the IMT/MIT phase transitions. Most importantly, the after-irradiation curves (dashed lines) lay between the curves before irradiation and are almost identical for temperatures at 168 K and below (solid lines). This implies that after irradiation, it is no longer possible to decide (by means of the filling factor) whether the film was in the heating or cooling branch. In this sense, laser irradiation above the power threshold erases the thermal history of the V_2O_3 thin film.

The most intriguing result of this study is that laser irradiation predominantly induces insulating domains in large amounts during cooling. Considering the laser spot

as a local heat source, it is not surprising that laser irradiation induces metallic domains since the metallic phase is the high-temperature phase of the Mott transition. Indeed, we observe this behavior during heating of the sample through the IMT. However, the predominant laser-induced creation of insulating domains during cooling is puzzling. In other words, why does the effect of laser irradiation depend on the thermal history? To answer this question, the thermodynamic nature of the MIT/IMT of the V_2O_3 thin film must be considered.

The thermodynamic description of V_2O_3 thin films is the subject of ongoing research [35–37]. The $R(T)$-hysteresis and the associated latent heat indicate a first-order phase transition. Moreover, it is recognized that at the MIT, three phase transitions are coupled: first, an electronic transition due to Mott-Hubbard charge carrier localization, second, a magnetic transition from a paramagnetic-to-antiferromagnetic state, and third, a structural transition from corundum to a monoclinic crystal structure. Simultaneous to the Mott-transition, there is the spontaneous separation in the metallic and insulating phases forming herringbone domains [33].

As indicated in Ref. [29], these characteristic herringbone domain pattern resembles the solutions of the Cahn-Larché equation describing a phase separation due to spinodal decomposition of an elastically stressed system [38]. Other studies also indicate that the IMT/MIT is associated with a spinodal instability [39, 40].

Due to the fundamental thermodynamic characteristics of a first-order phase transition, the V_2O_3 thin film is in a metastable superheated state during the IMT, and it is in a metastable supercooled state during the MIT. The most likely interpretation of our results is that the perturbation releases the V_2O_3 thin film from its metastable state, and when the laser spot moves to a new position, the thin film relaxes locally into a stable state.

The general details on how the laser spot on the thin film surface affects the metastability of V_2O_3 are elusive. As discussed above, laser-induced heating needs to be considered. The V_2O_3 thin film is thermally coupled via the sapphire substrate to the cold finger of the cryostat fixed at the set temperature. The focused laser spot raises locally the film temperature. Because the sapphire substrate has a high thermal conductance, the coupling of the V_2O_3 film to the thermal bath is expected to be strong. Consequently, the temperature distribution relaxes in a new steady state on a fast time scale when the laser spot position changes during the scanning procedure.

As a further contribution to the open question of the laser perturbation mechanism, we measured electrical transport properties during minor thermal cycles to investigate how heating affects a V_2O_3 thin film in the critical state at the MIT. This procedure emulates a heat source that changes the temperature gradually on a large length scale. A detailed description and discussion of these additional experiments can be found in Ref. [32] (Sec. IV). Although we found that a minor heating cycle can indeed increase the resistance, the effect is not strong enough to account for what we observed in the laser irradiation experiment. Hence, additional effects might be at play, for instance, a photoinduced change of the $3d$-orbital occupation could trigger the formation of metallic nanodroplets in the IMT [41].

To elaborate on the matter of metastability, we discuss a phenomenological numerical model. In a two-dimensional (2D) resistor network, each site can either be metallic or insulating, depending on the local temperature, which is updated at every simulation step. Solving Kirchhoff's laws, currents and voltages on each site are determined. A first-order Landau-type free energy functional provides stable and metastable states separated by a barrier. The laser irradiation is implemented in the model by decreasing the barrier height to drive transitions between insulating and metallic states. For each site, the escape from a metastable state was determined by comparing random numbers to Boltzmann factors with a constant number of iterations. If the escape criterion is fulfilled, the transition probability is given by a Boltzmann distribution; see Sec. V in Ref. [32] for details.

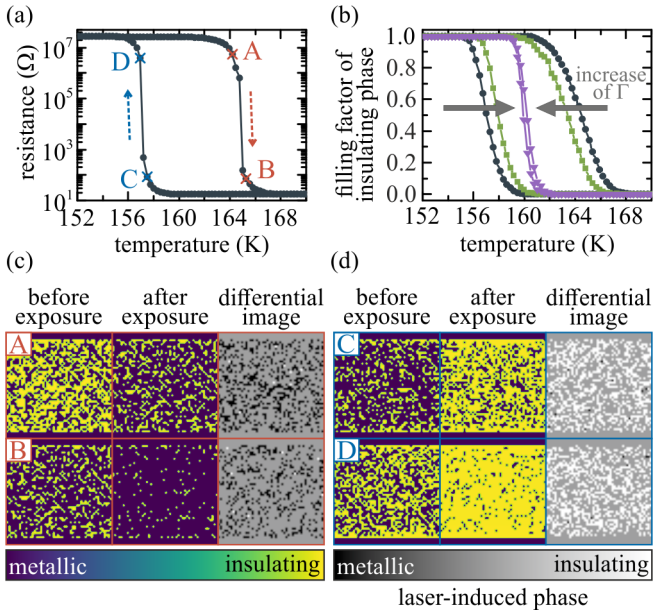


FIG. 3. Results of numerical simulations based on a 2D resistor network model. (a) $R(T)$ curves; arrows indicate heating (red) and cooling (blue) branches. (b) Filling factors of the insulating phase vs. T, for various values of laser intensity $\Gamma/k_B = 0$ (grey circles), 600 K (green squares) and 1200 K (purple triangles). (c) Selected network maps before laser exposure, after laser exposure with $\Gamma/k_B = 600$ K, and their corresponding differential images for two temperature values in the heating branch, as indicated with capital letters in (a). (d) same as in (c) – for the cooling branch.

Our model reproduces the hysteresis in the $R(T)$ curves, as shown in Fig. 3(a). Figure 3(b) shows the evolution of the filling factor of the insulating phase at different laser intensities. With increasing laser intensity the hysteresis is diminished, and eventually it is completely suppressed, similarly to the experimental results in Fig. 2(c). In Fig. 3(c) we present a simulation series of selected network maps before and after laser exposure with moderate laser intensity ($\Gamma/k_{\mathrm{B}} = 600\,\mathrm{K}$), and their corresponding differential images. For heating, the laser induces predominantly metallic sites (Fig. 3(c)), for cooling insulating sites (Fig. 3(d)). We note that during heating, the majority of sites goes into a metallic state (indicated by black squares in the differential maps), while a few sites revert back to an insulating state (indicated by white squares in the differential maps); this reproduces very well the experimental results. Moreover, this behavior reverses in the cooling branch (Fig. 3(d), again in agreement with experimental observations. So, according to the simulations, the laser irradiation enhances the process of relaxing the system from a metastable state.

In conclusion, we can state that a V_2O_3 thin film in the metastable state at the IMT/MIT is highly susceptible to a local perturbation by a focused laser beam at the sub-micrometer scale. Whether the laser perturbation predominantly creates a metallic or insulating phase depends on whether the film is in the heating or cooling branch. Our observations tell that the laser beam brings the system from a supercooled/superheated state to the equilibrium one, provided that the laser power is sufficient to overcome corresponding energy barriers. This implies, that laser scanning irradiation can be used to effectively erase thermal history and provides a novel method to reset memristive devices locally. Our experiments may also be considered as a clear indication that external stimuli on a strongly correlated thin film in a critical state can result in unexpected and presumably non-thermal effects. Non-thermal effects have been investigated in ultra-fast pump-probe experiments on VO_2 and V_2O_3 [41–45]. In contrast, in our experiment we have a quasi-static setting. The discoveries presented here invigorate the emerging field of neuromorphic computing and the research on strongly correlated materials out-of-equilibrium.

T.L. acknowledges support from the Cusanuswerk, Bischöfliche Studienförderung, F.T. acknowledges support from the Landesgraduiertenförderung Baden-Württemberg and M.R. acknowledges support from the French ANR "MoMA" project ANR-19-CE30-0020. This project has received funding from the European Union's Horizon Europe research and innovation programme under grant agreement No. 2031928 – "Highly Energy-Efficient Resistive Switching in Defect- and Strain- Engineered Mott Insulators for Neuromorphic Computing Applications". Views and opinions expressed are however those of the authors only and do not necessarily reflect those of the European union or the European research council. Work at University of California San Diego (UCSD) was supported through an Energy Frontier Research Center program funded by the US Department of Energy (DOE), Office of Science, Basic Energy Sciences, under Grant DE-SC0019273.

* stefan.guenon@uni-tuebingen.de

[1] I. K. Schuller, R. Stevens, R. Pino, and M. Pechan, Neuromorphic Computing – From Materials Research to Systems Architecture Roundtable, 10.2172/1283147 (2015).

[2] J. del Valle, J. G. Ramírez, M. J. Rozenberg, and I. K. Schuller, Challenges in materials and devices for resistive-switching-based neuromorphic computing, Journal of Applied Physics **124**, 211101 (2018).

[3] A. Hoffmann, S. Ramanathan, J. Grollier, A. D. Kent, M. J. Rozenberg, I. K. Schuller, O. G. Shpyrko, R. C. Dynes, Y. Fainman, A. Frano, E. E. Fullerton, G. Galli, V. Lomakin, S. P. Ong, A. K. Petford-Long, J. A. Schuller, M. D. Stiles, Y. Takamura, and Y. Zhu, Quantum materials for energy-efficient neuromorphic computing: Opportunities and challenges, APL Materials **10**, 070904 (2022).

[4] T. J. Park, S. Deng, S. Manna, A. N. M. N. Islam, H. Yu, Y. Yuan, D. D. Fong, A. A. Chubykin, A. Sengupta, S. K. R. S. Sankaranarayanan, and S. Ramanathan, Complex Oxides for Brain-Inspired Computing: A Review, Advanced Materials **35**, 2203352 (2022).

[5] F. J. Morin, Oxides Which Show a Metal-to-Insulator Transition at the Neel Temperature, Physical Review Letters **3**, 34 (1959).

[6] D. B. McWhan and J. P. Remeika, Metal-Insulator Transition in $(V_{1-x}Cr_x)_2O_3$, Physical Review B **2**, 3734 (1970).

[7] D. B. McWhan, A. Menth, J. P. Remeika, W. F. Brinkman, and T. M. Rice, Metal-insulator Transitions in Pure and Doped V_2O_3, Physical Review B **7**, 1920 (1973).

[8] A. Georges, G. Kotliar, W. Krauth, and M. J. Rozenberg, Dynamical mean-field theory of strongly correlated fermion systems and the limit of infinite dimensions, Reviews of Modern Physics **68**, 13 (1996).

[9] P. Limelette, A. Georges, D. Jerome, P. Wzietek, P. Metcalf, and J. M. Honig, Universality and Critical Behavior at the Mott Transition, Science **302**, 89 (2003).

[10] J. B. Torrance, P. Lacorre, A. I. Nazzal, E. J. Ansaldo, and C. Niedermayer, Systematic study of insulator-metal transitions in perovskites $RNiO_3$ (R=Pr,Nd,Sm,Eu) due to closing of charge-transfer gap, Physical Review B **45**, 8209 (1992).

[11] S. Catalano, M. Gibert, J. Fowlie, J. Íñiguez, J.-M. Triscone, and J. Kreisel, Rare-earth nickelates $RNiO_3$: thin films and heterostructures, Reports on Progress in Physics **81**, 046501 (2018).

[12] S. Biermann, A. Poteryaev, A. I. Lichtenstein, and A. Georges, Dynamical Singlets and Correlation-Assisted Peierls Transition in VO_2, Physical Review Letters **94**, 026404 (2005).

[13] M. Imada, A. Fujimori, and Y. Tokura, Metal-insulator

transitions, Reviews of Modern Physics **70**, 1039 (1998).
[14] Y. Zhou and S. Ramanathan, Mott Memory and Neuromorphic Devices, Proceedings of the IEEE **103**, 1289 (2015).
[15] B.-J. Kim, G. Seo, and Y. W. Lee, Bidirectional laser triggering of planar device based on vanadium dioxide thin film, Optics Express **22**, 9016 (2014).
[16] J. Kim, S. J. Jeong, B.-J. Kim, and Y. W. Lee, Laser-triggered current gating based on photothermal effect in VO_2 thin-film device using CO_2 laser, Applied Physics B **124**, 67 (2018).
[17] G. Seo, B.-J. Kim, Y. Wook Lee, and H.-T. Kim, Photo-Assisted Bistable Switching Using Mott Transition in Two-Terminal VO_2 Device, Applied Physics Letters **100**, 011908 (2012).
[18] G. Li, D. Xie, H. Zhong, Z. Zhang, X. Fu, Q. Zhou, Q. Li, H. Ni, J. Wang, E.-j. Guo, M. He, C. Wang, G. Yang, K. Jin, and C. Ge, Photo-Induced Non-Volatile VO_2 Phase Transition for Neuromorphic Ultraviolet Sensors, Nature Communications **13**, 1729 (2022).
[19] Y.-W. Lee, E.-S. Kim, B.-S. Shin, and S.-M. Lee, High-Performance Optical Gating in Junction Device based on Vanadium Dioxide Thin Film Grown by Sol-Gel Method, Journal of Electrical Engineering and Technology **7**, 784 (2012).
[20] G. Seo, B.-J. Kim, H.-T. Kim, and Y. W. Lee, Photo-Assisted Electrical Oscillation in Two-Terminal Device Based on Vanadium Dioxide Thin Film, Journal of Lightwave Technology **30**, 2718 (2012).
[21] T. Driscoll, H.-T. Kim, B.-G. Chae, M. D. Ventra, and D. N. Basov, Phase-transition driven memristive system, Applied Physics Letters **95**, 043503 (2009).
[22] A. Rana, C. Li, G. Koster, and H. Hilgenkamp, Resistive switching studies in VO_2 thin films, Scientific Reports **10**, 3293 (2020).
[23] X. Gao, C. M. M. Rosário, and H. Hilgenkamp, Multi-level operation in VO_2-based resistive switching devices, AIP Advances **12**, 015218 (2022).
[24] Y. Kalcheim, N. Butakov, N. M. Vargas, M.-H. Lee, J. del Valle, J. Trastoy, P. Salev, J. Schuller, and I. K. Schuller, Robust Coupling between Structural and Electronic Transitions in a Mott Material, Physical Review Letters **122**, 057601 (2019).
[25] B. A. Frandsen, Y. Kalcheim, I. Valmianski, A. S. McLeod, Z. Guguchia, S. C. Cheung, A. M. Hallas, M. N. Wilson, Y. Cai, G. M. Luke, Z. Salman, A. Suter, T. Prokscha, T. Murakami, H. Kageyama, D. N. Basov, I. K. Schuller, and Y. J. Uemura, Intertwined magnetic, structural, and electronic transitions in V_2O_3, Physical Review B **100**, 235136 (2019).
[26] J. Trastoy, A. Camjayi, J. del Valle, Y. Kalcheim, J.-P. Crocombette, D. A. Gilbert, J. A. Borchers, J. E. Villegas, D. Ravelosona, M. J. Rozenberg, and I. K. Schuller, Magnetic field frustration of the metal-insulator transition in V_2O_3, Physical Review B **101**, 245109 (2020).
[27] E. Barazani, D. Das, C. Huang, A. Rakshit, C. Saguy, P. Salev, J. del Valle, M. C. Toroker, I. K. Schuller, and Y. Kalcheim, Positive and Negative Pressure Regimes in Anisotropically Strained V_2O_3 Films, Advanced Functional Materials **33**, 2211801 (2023).
[28] M. K. Stewart, D. Brownstead, S. Wang, K. G. West, J. G. Ramírez, M. M. Qazilbash, N. B. Perkins, I. K. Schuller, and D. N. Basov, Insulator-to-Metal Transition and Correlated Metallic State of V_2O_3 Investigated by Optical Spectroscopy, Physical Review B **85**, 205113 (2012).
[29] M. Lange, S. Guénon, Y. Kalcheim, T. Luibrand, N. M. Vargas, D. Schwebius, R. Kleiner, I. K. Schuller, and D. Koelle, Imaging of Electrothermal Filament Formation in a Mott Insulator, Physical Review Applied **16**, 054027 (2021).
[30] M. M. Lange, S. Guénon, F. Lever, R. Kleiner, and D. Koelle, A High-Resolution Combined Scanning Laser and Widefield Polarizing Microscope for Imaging at Temperatures from 4 K to 300 K, Review of Scientific Instruments **88**, 123705 (2017).
[31] M. M. Lange, A High-Resolution Polarizing Microscope for Cryogenic Imaging: Development and Application to Investigations on Twin Walls in $SrTiO_3$ and the Metal-Insulator Transition in V_2O_3, Ph.D. thesis, Universität Tübingen (2018).
[32] See Supplemental Material at [URL] for details on the sample and measurement setup, a microbridge experiment, thresholds of laser scanning irradiation, analysis of thermal effects via minor loop measurements, and Mott resistor network simulation.
[33] A. S. McLeod, E. van Heumen, J. G. Ramírez, S. Wang, T. Saerbeck, S. Guénon, M. Goldflam, L. Anderegg, P. Kelly, A. Mueller, M. K. Liu, I. K. Schuller, and D. N. Basov, Nanotextured Phase Coexistence in the Correlated Insulator V_2O_3, Nature Physics **13**, 80 (2016).
[34] J. Schindelin, I. Arganda-Carreras, E. Frise, V. Kaynig, M. Longair, T. Pietzsch, S. Preibisch, C. Rueden, S. Saalfeld, B. Schmid, J.-Y. Tinevez, D. J. White, V. Hartenstein, K. Eliceiri, P. Tomancak, and A. Cardona, Fiji: an open-source platform for biological-image analysis, Nature Methods **9**, 676 (2012).
[35] C. Castellani, C. DiCastro, D. Feinberg, and J. Ranninger, New Model Hamiltonian for the Metal-Insulator Transition, Physical Review Letters **43**, 1957 (1979).
[36] G. Kotliar, E. Lange, and M. J. Rozenberg, Landau Theory of the Finite Temperature Mott Transition, Physical Review Letters **84**, 5180 (2000).
[37] M. I. Díaz, J. E. Han, and C. Aron, Electrically Driven Insulator-to-Metal Transition in a Correlated Insulator: Electronic Mechanism and Thermal Description, Physical Review B **107**, 195148 (2023).
[38] H. Garcke and U. Weikard, Numerical Approximation of the Cahn-Larché Equation, Numerische Mathematik **100**, 639 (2005).
[39] T. Bar, S. K. Choudhary, M. A. Ashraf, K. S. Sujith, S. Puri, S. Raj, and B. Bansal, Kinetic Spinodal Instabilities in the Mott Transition in V_2O_3: Evidence from Hysteresis Scaling and Dissipative Phase Ordering, Physical Review Letters **121**, 045701 (2018).
[40] S. Kundu, T. Bar, R. K. Nayak, and B. Bansal, Critical Slowing Down at the Abrupt Mott Transition: When the First-Order Phase Transition Becomes Zeroth Order and Looks Like Second Order, Physical Review Letters **124**, 095703 (2020).
[41] A. Ronchi, P. Homm, M. Menghini, P. Franceschini, F. Maccherozzi, F. Banfi, G. Ferrini, F. Cilento, F. Parmigiani, S. S. Dhesi, M. Fabrizio, J.-P. Locquet, and C. Giannetti, Early-Stage Dynamics of Metallic Droplets Embedded in the Nanotextured Mott Insulating Phase of V_2O_3, Physical Review B **100**, 075111 (2019).
[42] F. Giorgianni, J. Sakai, and S. Lupi, Overcoming the thermal regime for the electric-field driven Mott tran-

sition in vanadium sesquioxide, Nature Communications **10**, 1159 (2019).

[43] A. Cavalleri, C. Toth, C. W. Siders, J. A. Squier, F. Raksi, P. Forget, and J. C. Kieffer, Femtosecond Structural Dynamics in VO_2 during an Ultrafast Solid-Solid Phase Transition, Physical Review Letters **87**, 237401 (2001).

[44] S. Wall, S. Yang, L. Vidas, M. Chollet, J. M. Glownia, M. Kozina, T. Katayama, T. Henighan, M. Jiang, T. A. Miller, D. A. Reis, L. A. Boatner, O. Delaire, and M. Trigo, Ultrafast disordering of vanadium dimers in photoexcited VO_2, Science **362**, 572 (2018).

[45] M. R. Otto, L. P. René de Cotret, D. A. Valverde-Chavez, K. L. Tiwari, N. Émond, M. Chaker, D. G. Cooke, and B. J. Siwick, How optical excitation controls the structure and properties of vanadium dioxide, Proceedings of the National Academy of Sciences **116**, 450 (2018).